Cerebellar White Matter Abnormalities in Patients with Charcot-Marie-Tooth disease

Hyeon-Jin Kim
Ewha Womans University School of Medicine: Ewha Women's University College of Medicine and Graduate School of Medicine

Chang-Hyun Park
Ewha Womans University School of Medicine: Ewha Women's University College of Medicine and Graduate School of Medicine

Regina Eun-Young Kim
Korea University Anam Hospital

Sungeun Hwang
Ewha Womans University School of Medicine: Ewha Women's University College of Medicine and Graduate School of Medicine

Yun Seo Choi
Ewha Womans University School of Medicine: Ewha Women's University College of Medicine and Graduate School of Medicine

Sol-Ah Kim
Ewha Womans University School of Medicine: Ewha Women's University College of Medicine and Graduate School of Medicine

Jeong Hyun Yoo
Ewha Womans University School of Medicine: Ewha Women's University College of Medicine and Graduate School of Medicine

Ki Wha Chung
Kongju University: Kongju National University

Byung-Ok Choi
Sungkyunkwan University School of Medicine

Hyang Woon Lee (✉ leeh@ewha.ac.kr)
Ewha Womans University School of Medicine: Ewha Women's University College of Medicine and Graduate School of Medicine

---

Short Report

Keywords: Charcot-Marie-Tooth disease (CMT), Volumetry, Diffusion tensor imaging (DTI), White matter, Cerebellum, Ataxia

Posted Date: May 25th, 2021

DOI: https://doi.org/10.21203/rs.3.rs-410547/v1

Abstract

Charcot-Marie-Tooth disease (CMT) is a genetically heterogeneous hereditary peripheral neuropathy. Brain volumetry and diffusion tensor imaging (DTI) were performed in CMT patients with *PMP22* duplication, *MFN2*, *GJB1*, or *NEFL* mutations to investigate for structural changes of the cerebellum.

Volume in cerebellar white matter (WM) was significantly reduced in CMT patients with *NEFL* mutations. Abnormal DTI findings were observed in the superior, middle, and inferior cerebellar peduncles predominantly in *NEFL* mutations, and partly in *GJB1* mutations. Cerebellar ataxia was more prevalent in the *NEFL* mutation (72.7%) than *GJB1* mutation (9.1%), but not observed in other genotypic subtypes, which indicates that structural cerebellar abnormalities were associated with the presence of cerebellar ataxia. However, *NEFL* and *GJB1* mutations did not affect cerebellar gray matter (GM), and neither cerebellar GM nor WM abnormalities were observed in *PMP22* duplication or *MFN2* mutations. We found structural evidence of cerebellar WM abnormalities in CMT patients with *NEFL* and *GJB1* mutations and the association between cerebellar WM involvement and cerebellar ataxia in these genetic subtypes, especially in the *NEFL* subgroup. Therefore, we suggest that neuroimaging such as MRI volumetry or DTI in CMT patients could play an important role in detecting abnormalities of the cerebellar WM.

Introduction

Charcot-Marie-Tooth disease (CMT) is a hereditary peripheral neuropathy with clinical and genetic heterogeneities (Shy et al. 2002). Peripheral myelin protein 22 (*PMP22*) duplication is known to cause CMT1A, mitofusin 2 (*MFN2*) mutations cause CMT2A, and gap junction protein 1 (*GJB1*) mutations relevant with CMTX1 (DiVincenzo et al. 2014). Mutations in the neurofilament light chain polypeptide (*NEFL*) produce a variety of CMT phenotypic spectra including CMT1F, CMT2E, dominant intermediate CMT G (CMTDIG), and autosomal recessive CMT (Jordanova et al. 2003).

Cerebellar ataxia is one of the common symptoms of cerebellar dysfunction and manifests as an inability to coordinate balance and gait (Ferrarin et al. 2005). Cerebellar ataxia has been reported in some *NEFL* patients (Horga et al. 2017; Miltenberger-Miltenyi et al. 2007; Berciano et al. 2015; Yang et al. 2016; Yang et al. 2016; Lee et al. 2017). From the literature review, among 173 patients with *NEFL* mutations, ataxia was found in 22 patients and cerebellar atrophy in 4 patients (Horga et al. 2017). Although the patients have cerebellar ataxia, it is difficult to find cerebellar atrophy using brain MRI. There has been no report of volumetry or diffusion tensor imaging (DTI) studies other than MRI studies of the cerebellum in patients with *NEFL* mutations.

In this study, we used both volumetry and DTI to search for structural changes in the cerebellum in 47 controls and 47 CMT patients with mutations in various genes including *PMP22*, *MFN2*, *GJB1*, and *NEFL* mutations. Interestingly, we observed significant volumetric changes of the cerebellum in CMT patients especially with *NEFL* mutations, which was associated with the presence of cerebellar ataxia in this genetic subgroup.

Methods

Participants

We enrolled 94 study participants including 47 healthy controls and 47 CMT patients: 10 CMT1A patients with *PMP22* duplication, 15 CMT2A patients with *MFN2* mutations, 11 CMTX1 patients with *GJB1* mutations, and 11 CMT patients (3 CMT1F, 2 CMT2E, and 6 DMTDIG) with *NEFL* mutations (Table 1). Except one L312P *NEFL* patient having cerebellar atrophy, cerebellum showed normal findings in brain MRI. Determination of causative mutations and clinical assessments were performed as described previously (Lee et al. 2017). Especially, cerebellar ataxia was assessed by the Ataxia Clinical Assessment Index (Ferrarin et al. 2005).

MR volumetry and diffusion tensor imaging (DTI)

We performed 3-T MRI for volumetry and DTI with high resolution 3-dimensional T1-weighted images and diffusion-weighted EPI sequences (Philips Achieva v2.6, Best, Netherlands). The MRI processing consisted of AC-PC co-registration between T1-images, multimodal bias-correction, and applying a multi-label joint fusion algorithm. Using the BRAINSTools suite, the brain was divided into 217 sub-regions, which were then classified as either cerebral or cerebellar for further analysis. Finally, age and total intracranial volumes were adjusted to compare the WM and gray matter (GM) volumes. All volumetric data were processed through a fully automated procedure, BRAINS Auto-Workup (BAW) (Kim and Jonson 2014; Kim et al. 2015; Forbes et al. 2016), improved with SyN registration from the Advanced Normalization Toolkit in the BRAINSTools suite (https://github.com/BRAINSia/BRAINSTools) (Kim et al. 2015). The resulting data set of bias-corrected average T1 images were subsequently segmented for subcortical structures using an automated segmentation framework, ANTs MALF (Kim et al. 2015; Wang and Yushkevich 2013). Both of the raw data and the resulted segmentation were visually inspected for their validity.

DTI data were collected using the same parameters (TR 4500 ms, TE 68 ms, EoV RL 240 mm X AP 240 mm, FH 135 mm, matrix size 128 x 128 mm, 3 mm slice thickness, no gap, flip angle 90 degree, voxel size RL 2, AP 2, 32 directions with b-value 1000 sec/mm^2 and one null image with b-value 0 sec/mm^2, total diffusion gradient 80 mT/m, NSA=1, 45 slices in transverse plane) and analyzed using the tools included in FSL (http://fsl.fmrib.ox.ac.uk/fsl/) to compute DTI-derived measures including fractional anisotropy (FA), axial diffusivity (AD), and radial diffusivity (RD), as described elsewhere (Lee et al. 2017). The protocol for this study was approval by the Institutional Review Board, and informed consent was obtained from all patients and from parents of patients younger than 18 years of age.

Statistical analysis

We analyzed volumetric data using R software version 3.3. Whole cerebellar tissue and regional cerebellar volumes were standardized to the individual intracranial volume (ICV) to account for differences in head size. We performed all analysis of volume differences using % scale, volume per ICV in percentage (Kim

et al. 2015). Left- and right-side volumes of the cerebellum were combined. Comparison of cerebellar volumes between normal control and CMT for genetic subtypes was performed using ANOVA using age and sex as covariates.

The tract-based spatial statistics (TBSS) approach was used for voxelwise statistical analysis (Lee et al. 2017; Smith et al. 2006; Kim et al. 2014). We compared the DTI-derived measures between control and CMT groups with genetic subtypes by using the nonparametric permutation method, with the threshold-free cluster enhancement approach at $p < 0.05$ corrected for multiple comparisons. The fractional anisotropy (FA) and diffusivity measures of DTI were tested for correlation with clinical variables by using Spearman's rank correlation coefficients (r) (Lee et al. 2017; Kim et al. 2014).

Results

The clinical features and nerve conduction studies of the 47 CMT patients are shown in Table 1. CMT patients had muscle weakness and atrophy predominantly in the distal legs ranging from mild weakness to complete paralysis. Genetic mutations included eight *MFN2* mutations, seven *GJB1* mutations, and six *NEFL* mutations. CMT patients with *NEFL* and *GJB1* mutations exhibited diverse cerebellar involvements including cerebellar ataxia, dysarthria, dyssynergia, or dysmetria. Especially, the frequency of the cerebellar ataxia was high in patients with *NEFL* mutations (72.7%), compared to *GJB1* mutations (9.1%), *PMP22* duplication (0%), and MFN2 mutations (0%).

The mean volume proportion of cerebellar region was 3.08% (± 0.25, V/ICV) for normal controls while most of CMT groups showed lower cerebellar regional volumes (table 1). A linear regression model showed a significant difference of cerebellar GM and WM volumes in *NEFL* mutation group (Figure 1A and 1B). The difference of cerebellar WM in the *NEFL* subgroup compared with the control group remained significant even after multiple comparison adjustments (-0.151 ± 0.031, $p = 0.0083$). Cerebellar WM volume of *MFN2* revealed a nonsignificant tendency to be reduced (-0.051 ± 0.028, $p = 0.07$). However, there was no statistically significant cerebellar atrophy in the other genotypes (*PMP22* duplication, *MFN2* or *GJB1* mutation).

DTI of the cerebellum revealed significantly reduced FA and AD, and increased RD values most prominently in the *NEFL* genetic subgroup and mildly in *GJB1* subtype, but no changes in the other subgroups with *PMP22* duplication or *MFN2* mutation (Figure 1C). In the *NEFL* genetic subtype, DTI of the cerebellum revealed significantly reduced FA values in 90.9% of the voxels of the superior cerebellar peduncle (SCP), 63.4% of the middle cerebellar peduncle (MCP) voxels, and 92.0% of the inferior cerebellar peduncle (ICP) voxels (figure 1D). Similarly, significantly deceased AD values were found in 68.0%, 57.0%, and 57.4% of the voxels, and increased RD values in 79.7%, 40.1% and 90.9% of the voxels in the SCP, the MCP, and the ICP, respectively (figure 1E). In the case of *GJB1* mutation, reduced FA values were found in 24.3%, 14.9% and 0.4% of the voxels, and increased RD values in 41.4%, 18.3%, and 1.9% of the voxels of the SCP, the MCP, and the ICP, respectively. AD values were not different from those of healthy controls. Interestingly, manifestation of cerebellar ataxia was largely restricted to the *NEFL*

subgroup: it was observed clinically in 8 out of 11 CMT patients in the *NEFL* subgroup (72.7%) but in only one out of 11 CMT patients (9.1%) in the *GJB1* subgroup (Figure 1D and 1E). Thus, abnormal DTI findings in cerebellar WM tracts combined with reduced cerebellar WM volume occurred predominantly in the *NEFL* subgroup, the subtype associated with cerebellar ataxia symptoms.

Discussion

In this study, we found structural evidence of cerebellar WM abnormalities including reduced cerebellar WM in the *NEFL* mutation group by volumetry, and microstructural abnormalities of SCP, MCP, and ICP in the *NEFL* and *GJB1* subgroups by DTI. It has been reported that brain T1-weighted MR image in CMT patients with N98S NEFL mutation showed cerebellar atrophy (Smith et al. 2006). It was not clear, however, whether cerebellar atrophy could be a common feature seen in the *NEFL* mutation in the previous studies. We examined the MRI volumetry and DTI studies in CMT patients including *NEFL* mutations harboring various mutation sites. As a result, we confirmed that cerebellar atrophy is a common phenomenon observed in the *NEFL* mutation group. In our study, we proved that the *NEFL* mutations affect the WM of the cerebellum but not the GM. In addition, cerebellar ataxia, which is commonly manifested in patients with *NEFL* mutations, is not well observed in the other genetic mutations, such as *PMP22, MFN2*, except in one out of 11 patients with *GJB1* mutations. As far as our knowledge, this is the first report of volumetric and DTI study in CMT patients with *NEFL* mutations showing cerebellar WM abnormality.

According to literature review, in 173 patients with *NEFL* mutations, ataxia was found in 22 patients and cerebellar atrophy in 4 patients (Yang et al. 2016; Horga et al. 2017). This means that some *NEFL* patients showed only cerebellar ataxia without cerebellar atrophy. In the present study, cerebellar ataxia was found in 72.7% in the *NEFL* subgroup, but cerebellar atrophy was observed in only one patient with L312P *NEFL* mutation. This discrepancy may be due to the fact that ataxia caused by cerebellar dysfunction is an early symptom than cerebellar atrophy. Therefore, it is difficult to find cerebellar atrophy by routine brain MRI, and cerebellar involvements in *NEFL* patients may be underestimated. Interestingly, having a high proportion of voxels in SCP, MCP, and ICP with reduced FA and increased RD occurred in the *NEFL* mutation group associated with cerebellar ataxia.

In addition, we found DTI cerebellar abnormalities in the *GJB1* mutation group. One patient with C179X *GJB1* gene mutation showed cerebellar ataxia without cerebellar atrophy in brain MRI. DTI of the cerebellum showed moderately reduced FA values in 24.3% of the voxels of the SCP in *GJB1* group. Therefore, MRI volumetry or DTI can be helpful for early detection of cerebellar dysfunction in CMT patients with *NEFL* and/or *GJB1* mutations, especially in cases harboring cerebellar ataxia. In fact, *GJB1* has been reported to relate mitochondrial function in motor neurons in CNS (Abrams and Freidin 2015), and to be expressed in both Schwann cells and oligodendrocytes, the myelinating glia of the PNS and CNS, respectively (Wang et al. 2015).

Our findings provide structural evidence for cerebellar WM involvements in CMT patients with *NEFL* mutations investigated by MRI volumetry and DTI studies, which is related to the prevalent manifestation of cerebellar ataxia in this genetic subtype. This study also demonstrates that quantitative MRI such as volumetry and DTI can be useful for clinical characterization including future development of CNS involvement in CMT patients with diverse genetic abnormalities.

Declarations

Funding: This work was supported by grants of the Korea Health Technology R&D Project through the Korea Health Industry Development Institute (KHIDI), funded by the Ministry of Health & Welfare (HI14C1989), and the Basic Science Research Program through the National Research Foundation of Korea (NRF) funded by the Ministry of Education, Science and Technology (MSIT) (No. 2019M3C1B8090803 and 2020R1A2C2013216) to HWL, and by grants from the National Research Foundation (2020M3H4A1A03084600, and 2021R1A4A2001389) and the Korean Health Technology R&D Project, Ministry of Health and Welfare (HI14C3484 and HI20C0039), and by the National Institute of Health (R01NS094388) to BOC.

Conflicts of interest/Competing interests: None of the authors have any conflict of interests related to this study.

Availability of data and material: All of the raw and processed data for genetic and imaging analysis were stored and can be accessed in our laboratory which supervised by the corresponding authors, BOC and HWL, respectively.

Authors' contribution: Conceptualization: Byun-ok Choi, Hyang Woon Lee; Methodology: Chang-Hyun Park, Regina Eun-Young Kim, Sungeun Hwang, Yun Seo Choi, Sol-Ah Kim; Formal analysis and investigation: Chang-Hyun Park, Regina Eun-Young Kim; Writing - original draft preparation: Hyeon-Jin Kim, Chang-Hyun Park, Regina Eun-Young Kim; Writing - review and editing: Sungeun Hwang, Yun Seo Choi, Sol-Ah Kim, Byung-ok Choi, and Hyang Woon Lee; Funding acquisition: Byung-ok Choi, Hyang Woon Lee; Resources: Byung-ok Choi, Hyang Woon Lee; Supervision: Jeong Hyun Yoo, Ki Wha Chung

Ethics approval: The protocol for this study received approval by the Institutional Review Board.

Consent to participate: Informed consent was obtained from all individual participants included in this study and from parents of patients younger than 18 years of age.

Consent for publication: The authors affirm that human research participants provided informed consent for publication of the images in Figure 1c.

References

Abrams CK, Freidin M (2015) GJB1-associated X-linked Charcot-Marie-Tooth disease, a disorder affecting the central and pheripheral nervous systems. *Cell Tissue Res* 360:659-673.

Berciano J, García A, Peeters K, et al (2015) NEFL E396K mutation is associated with a novel dominant intermediate Charcot-Marie-Tooth disease phenotype. *J Neurol* 262:1289-1300.

DiVincenzo C, Elzinga CD, Medeiros AC, et al (2014) The allelic spectrum of Charcot-Marie-Tooth disease in over 17,000 individuals with neuropathy. *Mol Genet Genomic Med* 2:522-529.

Ferrarin M, Gironi M, Mendozzi L, Nemni R, Mazzoleni P, Rabuffetti M (2005) Procedure for the quantitative evaluation of motor disturbances in cerebellar ataxic patients. *Med Biol Eng Comput* 43:349-356.

Forbes JL, Kim EY, Paulsen JS, Johnson HJ (2016) An Open-Source Label Atlas Correction Tool and Preliminary Results on Huntingtons Disease Whole-Brain MRI Atlases. *Front Neuroinform* 10:1–11.

Horga A, Laurà M, Jaunmuktane Z, Jerath NU, Gonzalez MA, Polke JM, Poh R, Blake JC, Liu YT, Wiethoff S, Bettencourt C, Lunn MP, Manji H, Hanna MG, Houlden H, Brandner S, Züchner S, Shy M, Reilly MM (2017) Genetic and clinical characteristics of NEFL-related Charcot-Marie-Tooth disease. *J Neurol Neurosurg Psychiatry* 88:575-585.

Jordanova A, De Jonghe P, Boerkoel CF, et al (2003) Mutations in the neurofilament light chain gene (NEFL) cause early onset severe Charcot-Marie-Tooth disease. *Brain* 126:590-597.

Kim EY, Johnson HJ (2014) A robust segmentation pipeline for consistent trajectory estimation of HD gene positive individuals across multiple longitudinal MRI sites. *Soc Neurosci* 32:2014.

Kim SE, Lee JH, Chung HK, Lim SM, Lee HW (2014) Alterations in white matter microstructures and cognitive dysfunctions in benign childhood epilepsy with centrotemporal spikes. *Eur J Neurol* 21:708-717.

Kim EY, Lourens S, Long JD, Paulsen JS, Johnson HJ (2015) Preliminary Analysis Using Multi-atlas Labeling Algorithms for Tracing Longitudinal Change. *Front Neurosci* 9(242). doi:10.3389/fnins.2015.00242.

Lee M, Park CH, Chung HK, et al (2017) Cerebral white matter abnormalities in patients with Charcot-Marie-Tooth disease. *Ann Neurol* 81:147-151.

Miltenberger-Miltenyi G, Janecke AR, Wanschitz JV, et al (2007) Clinical and electrophysiological features in Charcot-Marie-Tooth disease with mutations in the NEFL gene. *Arch Neurol* 64:966-970.

Shy ME, Garbern JY, Kamholz J (2002) Hereditary motor and sensory neuropathies: a biological perspective. *Lancet Neurol* 1:110-118.

Smith SM, Jenkinson M, Johansen-Gerg H, et al (2006) Tract-based spatial statistics: voxelwise analysis of multi-subject diffusion data. *Neuroimage* 31:1487-1505.

Yang Y, Gu LQ, Burnette WB, Li J (2016) N98S mutation in NEFL gene is dominantly inherited with a phenotype of polyneuropathy and cerebellar atrophy. *J Neurol Sci* 365:46-47.

Wang H, Yushkevich P (2013) Multi-atlas segmentation with joint label fusion and corrective learning—an open source implementation. *Front Neuroinform* 7:27.

Wang W, Zhang F, Li L, Tang F, Siedlak SL, Fujioka H, et al (2015) MFN2 couples glutamate excitotoxicity and mitochondrial dysfunction in motor neurons. *J Biol Chem* 290:168-182.

Yang Y, Gu LQ, Burnette WB, Li J (2016) N98S mutation in NEFL gene is dominantly inherited with a phenotype of polyneuropathy and cerebellar atrophy. *J Neurol Sci* 365:46-47.

Tables

Table 1. Basic demographic and clinical characteristics of study population.

	Normal control	*PMP22 Duplication*	*MFN2 mutations*	*GJB1 mutations*	*NEFL Mutations*
Number	47	10	15	11	11
Female (%)	49	45	60	45	36
Age at exam (years)	37.5±14.6	42.0±14.7	31.9±13.6	39.4±16.5	39.5±11.8
Age at onset (years)	-	11.2±6.9	10.6±11.3	23.5±13.7	14.0±4.5
Muscle weakness	No	UL < LL[a]	UL < LL	UL < LL	UL < LL
Sensory loss	No	Yes	Yes	Yes	Yes
MRC[b] (arm)	5	3.9±0.3	1.6±1.7	3.8±0.9	2.1±0.7
MRC[c] (leg)	5	2.1±1.2	1.4±1.3	3.5±1.3	1.8±0.6
FDS[d]	0	2.0±1.1	3.9±2.2	2.3±1.0	3.0±1.0
CMTNS v2[e]	0	14.3±5.5	18.7±8.9	12.6±6.3	14.7±5.7
Cerebellar ataxia	0	0	0	1 (9.1%)	8 (72.7%)
Peripheral ulnar nerve conduction studies					
CMAP[f] (mV)	15.9±2.8	6.6±3.5	7.2±6.0	9.3±3.0	5.8±4.8
MNCV[g] (m/s)	61.2±3.2	19.6±3.9	52.3±8.4	43.3±9.0	36.0±9.0
SNAP[h] (uV)	23.1±7.2	5.2±1.7	8.4±4.8	5.8±3.3	4.3±2.1
SNCV[i] (m/s)	51.6±2.5	21.3±4.8	32.9±5.8	30.5±3.2	36.3±3.8

[a]UL < LL, upper limb weakness < lower limb weakness; [b]MRC (arm), medical research counsel for motor weakness from finger abduction; [c]MRC (leg), medical research counsel for motor weakness from ankle dorsiflexion; [d]FDS, functional disability scale; [e]CMTNS v2, Charcot-Marie-Tooth neuropathy score version 2; [f]CMAP, compound muscle action potential; [g]MNCV, motor nerve conduction velocity; [h]SNAP, sensory nerve action potential; [i]SNCV, sensory nerve conduction velocity.

Normal NCV values: ulnar motor nerve, ≥51.1 m/s; ulnar sensory nerve, ≥37.5 m/s. Normal amplitude values: ulnar motor nerve, ≥8 mV; ulnar sensory nerve, ≥7.9 □.

Figures

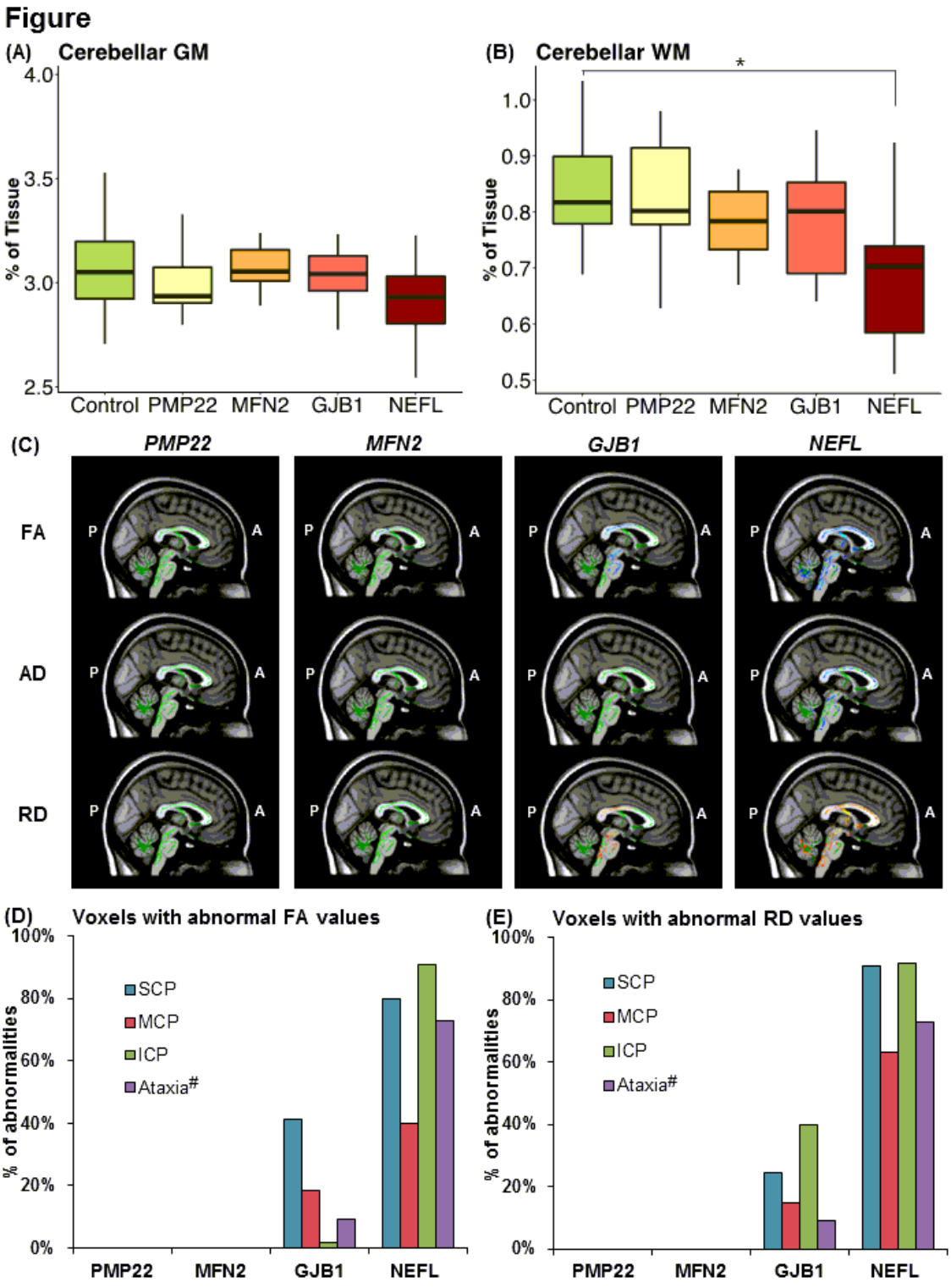

Figure 1

Volumetric and DTI findings in different genetic subtypes of CMT patients. CMT patients with NEFL genetic mutations demonstrate distinct decreased volumetric changes in cerebellar white matter (WM), but not cerebellar gray matter (GM), while neither cerebellar GM or WM changes were observed in the subgroups with PMP22 duplication, MFN2 or GJB1 mutations (A and B). DTI abnormalities including reduced FA and AD, and increased RD values were observed mostly in the genetic subgroup with NEFL

mutations (C). DTI abnormalities were found in major cerebellar WM tracts including the superior cerebellar peduncle (SCP), the middle cerebellar peduncle (MCP), and the inferior cerebellar peduncle (ICP), predominantly in the NEFL subgroup, but also in the GJB1 subgroup. Interestingly, having a high percentage of voxels of the SCP, the MCP, and the ICP with reduced FA and increased RD occurred in the NEFL genetic subgroup, which is the subgroup associated with cerebellar ataxia (D, E). Asterisk (*) indicate $p < 0.05$.